remote sensing

MDPI

Article

Evaluation of Ecological Environment Quality Using an Improved Remote Sensing Ecological Index Model

Yanan Liu, Wanlin Xiang *, Pingbo Hu, Peng Gao and Ai Zhang

School of Geomatics and Urban Spatial Informatics, Beijing University of Civil Engineering and Architecture, Beijing 100044, China; liuyanan@bucea.edu.cn (Y.L.); hupb@whu.edu.cn (P.H.); 2108570022088@stu.bucea.edu.cn (P.G.); 2108570023082@stu.bucea.edu.cn (A.Z.)

* Correspondence: 2108160222013@stu.bucea.edu.cn

Abstract: The Remote Sensing Ecological Index (***RSEI***) model is widely used for large-scale, rapid Ecological Environment Quality (***EEQ***) assessment. However, both the ***RSEI*** and its improved models have limitations in explaining the ***EEQ*** with only two-dimensional (2D) factors, resulting in inaccurate evaluation results. Incorporating more comprehensive, three-dimensional (3D) ecological information poses challenges for maintaining stability in large-scale monitoring, using traditional weighting methods like the Principal Component Analysis (***PCA***). This study introduces an Improved Remote Sensing Ecological Index (***IRSEI***) model that integrates 2D (normalized difference vegetation factor, normalized difference built-up and soil factor, heat factor, wetness, difference factor for air quality) and 3D (comprehensive vegetation factor) ecological factors for enhanced ***EEQ*** monitoring. The model employs a combined subjective–objective weighting approach, utilizing principal components and hierarchical analysis under minimum entropy theory. A comparative analysis of ***IRSEI*** and ***RSEI*** in Miyun, a representative study area, reveals a strong correlation and consistent monitoring trends. By incorporating air quality and 3D ecological factors, ***IRSEI*** provides a more accurate and detailed ***EEQ*** assessment, better aligning with ground truth observations from Google Earth satellite imagery.

Keywords: ecological environments; remote sensing ecological index; large-scale; 3D ecological factors; subjective and objective weights determination

Citation: Liu, Y.; Xiang, W.; Hu, P.; Gao, P.; Zhang, A. Evaluation of Ecological Environment Quality Using an Improved Remote Sensing Ecological Index Model. *Remote Sens.* **2024**, *16*, 3485. https://doi.org/10.3390/rs16183485

Academic Editor: Daniele Oxoli

Received: 1 August 2024
Revised: 14 September 2024
Accepted: 18 September 2024
Published: 20 September 2024

1. Introduction

The continuous development of society and increasing urbanization have greatly impacted the ecological space in urban areas [1], and many regional and global ecological problems are becoming more prominent, such as vegetation degradation [2], urban heat islands [3], and air pollution [4]. Therefore, the efficient, comprehensive, and accurate monitoring and assessment of regional ecological environments is crucial. ***EEQ*** monitoring using remote sensing data (imagery) has gradually become a common and efficient research method [5]. Studies [6–9] have primarily used a single 2D factor to evaluate the ecological environment status. However, the ecological environment is composed of multiple elements, and the assessment of a single ecological factor can only explain the ecological characteristics in one direction and cannot comprehensively reflect the ecological environment's status [10]. In recent years, researchers have explored the ***EEQ*** assessment by coupling several individual ecological indices, which can be divided into three main categories: the ecological index (***EI***) model; the remote sensing ecological index (***RSEI***) model; and other ecological environment models [11].

The EI index model, which aggregates the biological abundance, vegetation coverage, water network density, land degradation, and environmental quality, is the most widely used ecological environment evaluation index by the Ministry of Ecology and Environmental Protection of China [12]. It has been widely applied for regional ***EEQ*** assessment in China [13–15]. Based on the ***EI*** model, Ouyang et al. [16] subdivided the six ecological factors into 20 sub-indicators, and the weights were calculated using the hierarchical analysis

method, making the evaluation results more precise. Li et al. [17] selected the ecological factors needed in the inverse EI model based on the ***GEE*** platform, such as ***MODIS*** data, Landsat data, and night-time lighting data, and introduced a humidity factor to generate a new ecological index (***NEI***) model. However, the ***EI*** model relies on annual statistical or land use and land cover data, which are difficult to obtain, and the results must be divided along the administrative boundaries, which goes against natural ecological laws. Moreover, the weights and evaluation units are difficult to obtain and not universal.

The widely used ***RSEI*** model was first proposed by Xu [18] and it combined four factors including dryness, greenness, heat, and moisture with the principal component analysis (***PCA***) method. The ***RSEI*** model can reflect the pressure of human activities on the environment, the response to climate change, and changes in environmental conditions [19–22]. In recent years, research on improving ***RSEI*** has mainly been reflected in the selection of variable factors and the stable solution of the model. For the former, the ecological factors deriving from remote sensing imagery are usually added or substituted. For example, the mine-specific eco-environment index model was constructed by adding the atmospheric environment and mining scale [23]. The modified remotely sensed ecological index was constructed by introducing the landscape diversity index to evaluate oasis ecology [24], and the comprehensive salinity index and the remotely sensed water network density estimation model were constructed to evaluate the ecological quality of the northwest arid zone [25]. For the latter, the entropy weighting method was used instead of ***PCA*** to construct the ***RSEI*** model that considers all ecological factors [26]. Studies have proven that the first principal component of ***PCA*** selected for the ***RSEI*** model cannot fully characterize ecological features; therefore, the first three principal components of PCA are used [27]. Moreover, the nonlinear kernel principal component method has also been used to construct nonlinear remote sensing ecological indices [28]. The ***RSEI*** model is conducive to quantitatively evaluating ***EEQ*** changes at the regional scale, and its reliability and credibility have been verified. Furthermore, its ***EEQ*** results can be visualized, scaled, and compared at different spatiotemporal scales. However, the construction of an ***RSEI*** model is complex and subjective, and the ***EEQ*** is prone to be the opposite when using ***PCA***. In particular, it is only suitable for a small number of calculations and is not suitable for long-term sequence and batch operations [29]. Most importantly, in large-scale ***EEQ*** assessment, the ***RSEI*** and its improved models only utilize two-dimensional ecological factors and have not considered vertical three-dimensional information [30].

Other ecological models include the pressure-state-response (***PSR***) model [31,32], the InVEST model [33], and so on. These ecological evaluation models have made important contributions to ***EEQ*** evaluation [34–37]. Ashraf et al. [38] researched the development of the Spatial Ecosystem Health Index (***SEHI***), including indicator weights and selection using the remotely sensed Pressure-State-Response (***PSR***) framework, the Hierarchical Analysis Method (***AHP***), and the Principal Component Analysis (***PCA***) in 1990, 2003, 2013, and 2021, respectively. Based on the land use and land cover (***LULC***) data in 2000, 2010, and 2020, Li et al. [39] first predicted the trends and results in 2030. Then, the habitat quality was evaluated from 2000 to 2030 using the InVEST model, which showed that habitat quality was highly correlated with land use change. However, most of these models rely computationally on hard-to-access data such as ***LULC***, and these models often focus on specific ecological services or stressors, which may lead to the neglect of other ecosystem functions and services. Moreover, ecosystems are multidimensional representations of the real world, and the 2D expression of these models may not fully account for these complex interactions.

The objectives of this study were as follows: (1) to integrate 2D and 3D ecological factors for ***EEQ*** evaluation, enabling a transition from 2D to 3D ecological monitoring across large regions, (2) to incorporate air quality as a factor in the proposed ***IRSEI*** model for more comprehensive ecological environment monitoring, and (3) to employ a combined subjective–objective weighting model to assess ecological quality, enhancing the stability and rationality of ***EEQ*** results.

2. Materials

2.1. Study Area

This study selects a well famous ecological support district, named Miyun (Figure 1), located in northeast Beijing (40°13′N–40°48′N, 116°40′E–117°30′E). It is surrounded by mountains and rolling peaks in the east, north, and west. The ancient Great Wall stretches over the mountains. In the middle is the rippling Miyun Reservoir, and in the southwest is the flooded alluvial plain. It falls under the warm temperate monsoon continental semi-moist and semi-arid climate, governed by the high-pressure systems of Siberia and Mongolia in winter and influenced by continental low pressure and Pacific Ocean high pressure in summer. It experiences four distinct seasons with noticeable variations in dryness, wetness, coldness, and warmth. The average temperature in January is −3.5 °C, while in July it is 26.8 °C, with an annual precipitation of around 577 mm. As the most important water source in Beijing, it has the largest forest, the best wetland resources, and the richest biodiversity. In addition, the functional zoning distribution from A1 to A5 can carry different functions [40].

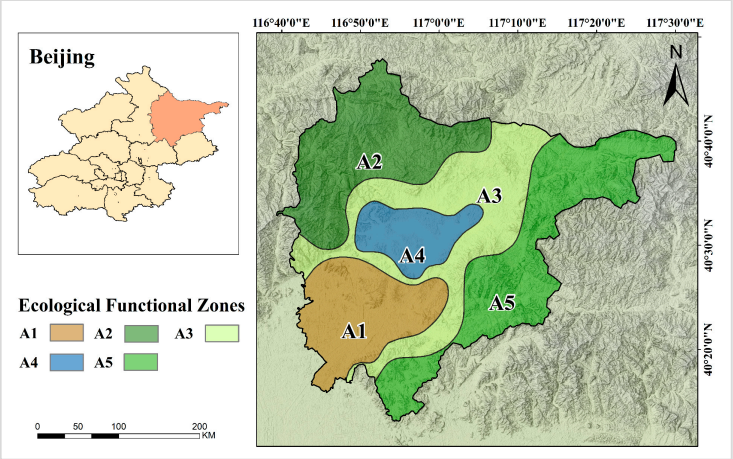

Figure 1. Overview of the study area with different ecological function zones. A1: core zone for comprehensive development; A2: ecological connotation zone; A3: ecological conservation zone; A4: water conservation zone; A5: green development zone.

2.2. Data and Pre-Processing

The remote sensing data used in this study are 2D multispectral remote sensing images and 3D spaceborne laser scanning point clouds.

(1) Multispectral remote-sensing images (2D)

These used remote sensing imagery are Landsat8 OLI imagery, obtained from the United States Geological Survey (***USGS***) [41]. Owing to the vegetation growth condition, we selected the Landsat8 OLI image on 18 September 2019, with a spatial resolution of 30 m × 30 m and cloud content of 0.01%. The pre-processing is accomplished by Google Earth Engine (GEE) including radiometric calibration, atmospheric correction, stitching, and cropping, and these images can be further used to calculate 2D ecological factors.

(2) Laser-scanning point cloud (3D)

The three-dimensional (3D) indicators, generated from the global ecosystem dynamics investigation (***GEDI***) and the Ice, Cloud, and Land Elevation Satellite-2 (ICESat-2), can provide more detailed and accurate results, as well as new ecological insights; therefore, they can be effectively used to improve ecological models for large-scale ecosystem investigations. The adopted 3D indices used in the proposed method are calculated from the 3D products (Guo et al. 2021). These 3D data were combined with inverse vegetation canopy height data using neural network-guided interpolation [42]. The resulting products have

no saturation effect in areas with a high forest canopy and can be used to reflect vegetation vertical structure for regional ecological assessment.

3. Methods

The proposed methodological framework (Figure 2) encompasses three key components: ecological factor calculations (Section 3.1), model construction (Section 3.2), and model validation (Section 3.3). The 2D and 3D ecological factors were initially calculated from the Landsat8 OLI image, ICESat-2, and ***GEDI*** data. Subsequently, the ***IRSEI*** model for ***EEQ*** assessment was constructed through a combined subjective–objective approach (***PCA-AHP***). Finally, the performance of the newly proposed ***IRSEI*** model was evaluated.

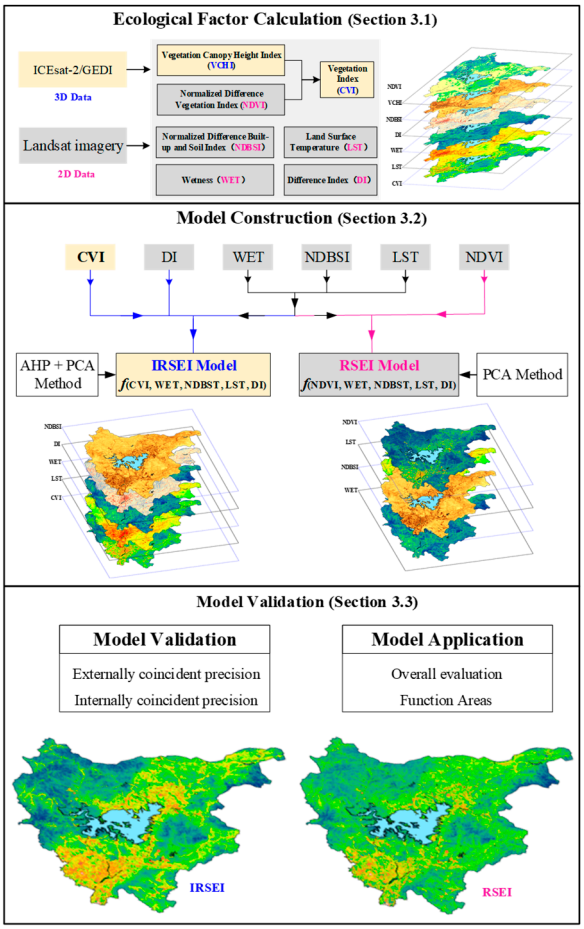

Figure 2. The pipeline of the proposed method.

3.1. Ecological Factors Calculation

The ***IRSEI*** model incorporates vegetation, humidity, aridity, heat, and air quality as ecological factors, while the original ***RSEI*** model considers vegetation, humidity, aridity, and heat factors. When these ecological factors are calculated, a normalization process should be performed.

(1) Vegetation factor

The vegetation factor serves as a crucial indicator in assessing the quality status of the regional ecological environment. Here, a new Comprehensive Vegetation Index (***CVI***) was introduced, which incorporated 2D planar features (***NDVI***) and 3D vertical distribution information (***CVHI***). As the significant differences between the ***NDVI*** and ***CVHI***, the non-dimensional treatment is adopted, and the final formula is expressed as follows:

$$CVI = w_1 \cdot NDVI + w_2 \cdot CVHI \quad (1)$$

where ***NDVI*** is the normalized difference vegetation index. The ***CVHI*** [42] is the vegetation canopy height index, which is the 3D canopy height data acquired from the ***GEDI*** and ***ICESat***-2. The linear model, where the coefficients w_1 and w_2 are set to 0.5 based on prior experience, was used. Specifically, the three ecological factors were normalized to scale their values between 0 and 1.

(2) Wetness factor

The land surface moisture reflects the moisture content of water bodies, soil, and vegetation, and is closely related to ecology [22]. According to previous studies [43,44], the wetness can be obtained by inverting the bands and can be calculated by

$$\begin{aligned} WET(OLI) = \quad & 0.1511 \times \rho_{blue} + 0.1973 \times \rho_{Green} + 0.3283 \times \rho_{\mathrm{Red}} + \\ & 0.3407 \times \rho_{NIR} - 0.7117 \times \rho_{SWIR1} - 0.4559 \times \rho_{SWIR2} \end{aligned} \quad (2)$$

where ***WET*** (***OLI***) is applied to Landsat ***OLI*** images. The variables ρ_{blue}, ρ_{Green}, ρ_{Red}, ρ_{NIR}, ρ_{SWIR1}, and ρ_{SWIR2} are the reflectances of bands 2, 3, 4, 5, 6, and 7 of the ***OLI*** images, respectively.

(3) Dryness factor

The dryness factor responds to the dryness of the ground surface, which influences some ecological phenomena. The dryness factor is expressed by the bare soil index (SI), but in the regional environment, part of the built land also causes the surface to "dry out". Therefore, ***SI*** and the building index (***IBI***) were chosen to express the dryness factor (***NDBSI***) with the following formulas [22]:

$$NDBSI = \frac{SI + IBI}{2} \quad (3)$$

$$SI = \frac{(\rho_{SWIR1} + \rho_{\mathrm{Red}}) - (\rho_{NIR} + \rho_{blue})}{(\rho_{SWIR1} + \rho_{\mathrm{Red}}) + (\rho_{NIR} + \rho_{blue})} \quad (4)$$

$$IBI = \frac{2\rho_{SWIR1}/(\rho_{SWIR1} + \rho_{NIR}) - [\rho_{NIR}/(\rho_{NIR} + \rho_{\mathrm{Red}}) + \rho_{Green}/(\rho_{Green} + \rho_{SWIR1})]}{2\rho_{SWIR1}/(\rho_{SWIR1} + \rho_{NIR}) + [\rho_{NIR}/(\rho_{NIR} + \rho_{\mathrm{Red}}) + \rho_{Green}/(\rho_{Green} + \rho_{SWIR1})]} \quad (5)$$

where ρ_{blue}, ρ_{Green}, ρ_{Red}, ρ_{NIR}, and ρ_{SWIR1} refer to the reflectance of the 1st, 2nd, 3rd, 4th, 5th, and each band of the TM image, and the reflectance of the 2nd, 3rd, 4th, 5th, and 6th bands of the ***OLI*** image, respectively.

(4) Heat factor

Land Surface Temperature (***LST***) is the most direct indicator of heat and is frequently employed in ecological quality assessments [25]. The ***LST***, serving as the heat factor in this study, is calculated as follows:

$$L = gain \times DN + bias \quad (6)$$

$$T = K_2 / \ln(K_1/L + 1) \quad (7)$$

$$LST = T/[1 + (\lambda \cdot T/\rho) \ln \varepsilon] \quad (8)$$

where ***L*** is the temperature value of the thermal infrared band; gain is the gain value; ***DN*** is the gray value of the pixel; bias is the bias value; T is the temperature value at the sensor; $\boldsymbol{K}_1$ = 774.89 W/(m^2·sr·μm); $\boldsymbol{K}_2$ = 1321.08 k; λ is the central wavelength of the thermal infrared band; $\boldsymbol{\rho}$ is 1.438 × 10^{-2} K; and ε is the specific emissivity of ground objects estimated by the Sobrino model.

(5) Difference factor for air quality

The particulate matter, a large proportion of dust, is the chief pollutant of the atmosphere pollution in Beijing. According to the PM2.5 of particles, the reflectivity of the red

band increases, and the reflectivity of the near-infrared band decreases [23]. Thus, the difference index (***DI***) was constructed to characterize the air quality:

$$DI = \rho_{red} - \rho_{nir} \tag{9}$$

where $\boldsymbol{\rho}_{\mathrm{red}}$ and $\boldsymbol{\rho}_{\mathrm{nir}}$ are the surface reflectance in the near-infrared and red bands, respectively.

3.2. Model Construction

Two ecological models, that are the proposed ***IRSEI*** and common ***RSEI*** model, were constructed for EEQ evaluation with the following extracted ecological factors: ***NDVI***, ***CVI***, ***WET***, ***NDBSI***, ***LST***, and ***DI***.

(1) ***IRSEI*** model

The proposed ***IRSEI*** model, which combines 2D and 3D ecological factors is organized as follows:

$$IRSEI = f(CVI, WET, NDBSI, LST, DI) = \sum_{i=1}^{n}(W_i \times K_i) \tag{10}$$

where n denotes the number of extracted ecological factors; $\boldsymbol{W}_{\mathrm{i}}$ and $\boldsymbol{K}_{\mathrm{i}}$ are the weight and index values of the *i*-th ecological factor, respectively.

To achieve the final ***IRSEI*** model, the PCA approach is frequently used to estimate the weights, which can downscale the regional ecological environment with multiple factors. However, the impact of different evaluation factors on actual environmental problems is ignored. In the study of Xu et al. [45], it was shown that the first component of PCA has obvious ecological benefits, while the other components do not have clear ecological meanings. Therefore, when there is a situation where the contribution rate of the first component is low, the single use of PCA analysis will lose a large amount of data [46]. In addition, AHP is a method used for subjectively determining weights, enabling the quantification of expert a priori knowledge, and facilitating a comprehensive evaluation of multiple indicators. However, the results of AHP tend to be overly subjective and may overlook the information inherent in the data itself [47].

Therefore, a hybrid method/model (PCA-AHP) is proposed for the new ***IRSEI***, which can fix the weights ($\boldsymbol{W}_{\mathrm{i}}$) by combining objective analysis (PCA) and subjective analysis (hierarchical analysis; AHP).

Specifically, for the weight of each ecological factor ($\boldsymbol{W}_{\mathrm{i}}$), we first assumed that $\boldsymbol{W}_{1\mathrm{i}}$ and $\boldsymbol{W}_{2\mathrm{i}}$ are subjective and objective weights, which can be calculated using the PCA and AHP methods, respectively. Using the minimum information entropy and Lagrange's mean theorem, the final weight ($\boldsymbol{W}_{\mathrm{i}}$) can be expressed as:

$$\min F = \sum_{i=1}^{n} W_i(\ln W_i - \ln W_{1i}) + \sum_{i=1}^{n} W_i(\ln W_i - \ln W_{2i}) \tag{11}$$

$$s \cdot t \sum_{i=1}^{n} W_i = 1 (W_i > 0, i = 1, 2, \ldots n) \tag{12}$$

Also, using the Lagrangian median theorem, it is known that:

$$W_i = \frac{\sqrt{W_{1i} W_{2i}}}{\sum_{i=1}^{n} \sqrt{W_{1i} W_{2i}}} (i = 1, 2, \ldots n) \tag{13}$$

where ***W***i is the weight of the PCA–AHP hybrid model and ***i*** is the ***i***-th factor.

(2) ***RSEI*** model

The common ***RSEI*** model is constructed with 2D ecological factors, which are given by

$$RSEI = f(NDVI, WET, NDBSI, LST) \tag{14}$$

To obtain the ***RSEI*** model, the PCA method, which can effectively remove redundant information, is utilized, and the first component of PCA (PC_1) is selected for ***RSEI*** [18,45,48]. Finally, the model can be expressed as:

$$RSEI = 1 - PC_1(NDVI, WET, NDBSI, LST) \quad (15)$$

3.3. Model Validation

To evaluate the performance of the two models, field measurements and the commonly used average degree of correlation were used. Directly assessing model accuracy using extensive field measurements was challenging [49]. Thus, high-resolution remote sensing images from Google Earth (***GE***) were commonly used to validate ***EEQ*** accuracy [50–52]. To this end, we could randomly select checkpoints over the experimental areas, and the ***EEQ*** values of each selected sample were then compared to corresponding ecological performance as visually assessed from the ***GE*** images. Table 1, based on References [22,25,26], outlines the ***EEQ*** and referenced performance criteria.

Table 1. The classification and description of EEQ.

Grade	Values	Ecological Performance
Excellent	[1, 0.8)	High-vegetation cover, good natural conditions, and stable ecosystems.
Good	[0.8, 0.6)	Good natural conditions and good vegetation cover for human life.
Moderate	[0.6, 0.4)	Vegetation cover is medium and more suitable for human life.
Fair	[0.4, 0.2)	Vegetation cover is poor and arid and there are limiting factors for human life.
Poor	[0.2, 0]	Low vegetation cover, harsh conditions, and restrictions on human life

The average degree of correlation, that is the internal plausibility of the selected ecological factors, was calculated for model validation, which indicates the overall representativeness of the ***IRSEI*** and the correlation among the various indicators [23]. The average degree of correlation can be expressed as follows:

$$\overline{R} = \sum_{i=1}^{n} \left(\frac{|R_i|}{n} \right) \quad (16)$$

where ***n*** is the number of ecological factors, and R_i is the correlation coefficient between any two ecological indicators.

4. Results

4.1. Results of Calculated Factors

The calculated factors (***NDVI***, ***WET***, ***CVI***, ***NDBSI***, ***DI***, and ***LST***) are visualized in Figure 3. Their respective maximum values are 0.863, 0.726, 0.616, 0.449, 0.563, and 0.402.

As seen in Figure 3, ecological factors (***NDVI***, ***CVI***, and ***WET***) that have a positive impact on EEQ have smaller values in areas with greater human disturbance (e.g., urban areas), and larger values in places with better ecology (e.g., forests), while the opposite is true for the negative ecological factors. The recently introduced 3D ecological factor, ***CVI***, and the conventional 2D ecological factor, ***NDVI***, share a similar overall trend but exhibit distinctions in detail. ***CVI*** integrates the 3D parameters of vegetation, facilitating a more distinct separation of vegetation compared to traditional ***NDVI***.

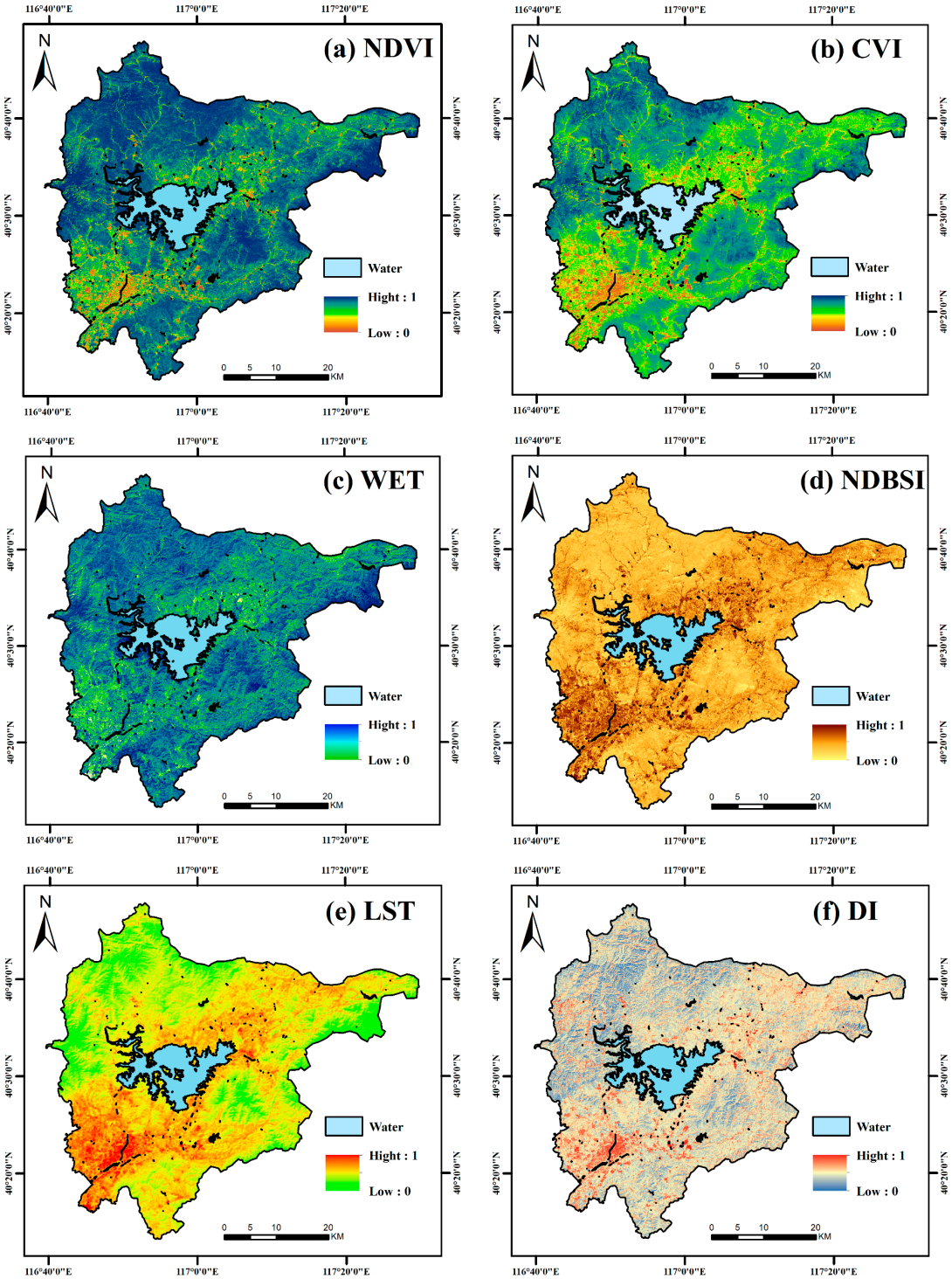

Figure 3. Map of the calculated ecological factors.

4.2. Results of the Two Constructed Models

To obtain the final models, the PCA method was used to generate the ***RSEI*** model (4 factors), whereas both PCA and AHP methods were adopted for the ***IRSEI*** model (5 factors). The results for each principal component calculated by ***PCA*** are listed in Table 2.

Table 2. Contributions of the model's ecological factors by ***PCA*** method.

Model	Factors	PC_1	PC_2	PC_3	PC_4	PC_5
IRSEI (Proposed)	**CVI**	0.703	0.609	0.257	0.260	0.019
	WET	0.382	−0.616	0.152	0.212	0.638
	NDBSI	−0.491	0.463	0.235	−0.041	0.698
	LST	−0.288	0.005	−0.165	0.938	−0.096
	DI	−0.188	−0.188	0.910	0.071	−0.310
	EV [1]	0.032	0.008	0.005	0.002	0
	pEV (%) [2]	68.169	17.266	10.257	3.286	1.023
RSEI (Original)	**NDVI**	0.337	−0.384	0.550	0.661	
	WET	0.572	0.575	−0.429	0.399	
	NDBSI	−0.671	−0.057	−0.385	0.630	
	LST	−0.330	0.721	0.604	0.083	
	EV [1]	0.021	0.002	0.001	0	
	pEV (%) [2]	83.25	9.56	6.00	1.150	

[1] **EV** is the eigenvalue; [2] **pEV** is the contribution of the eigenvalue; PC_i is the ***i***-th component of ***PCA***.

As can be seen from Table 2 that only the first principal component (PC_1) has real ecological significance and integrates the main information (68.619%, 83.25%) for both the ***RSEI*** and ***IRSEI*** models, regardless of whether 4 or 5 ecological factors are considered. In PC_1, the ecological factors that are beneficial to the ***EEQ*** show positive values, while detrimental ones are negative. This illustrates its stability for the first principal component PC_1. In addition, among other principal components ($PC_{2–5}$), their values are either positive or negative, making it difficult to distinguish the actual ecological meaning. Therefore, it is not suitable for us to adopt $PC_{2–5}$ for ***EEQ*** evaluation except the PC_1. Moreover, in the PC_1 component of the ***IRSEI*** model, ***CVI*** has the largest value (0.703), which indicates that vegetation plays a decisive role in the evaluation of ecological environment quality. This result is consistent with similar studies [11,53,54]. Furthermore, the proportion of PC_1 in the ***IRSEI*** model reached 68.169%, while other principal components showed both positive or negative values, making it difficult to distinguish their actual ecological significance.

Thus, it is not suitable to solely use ***PCA*** to generate the ***IRSEI*** model and assess the ***EEQ***, as it results in the loss of 31.831% of the information. To overcome this key issue, the AHP analysis method, incorporating expert prior knowledge, was employed to refine the proposed ***IRSEI*** model; the details are listed in Table 3. It is generally believed that a ***CR*** less than 0.1 indicates compliance with the consistency test, indicating that the constructed model is reliable [55].

Table 3. The weights for the ***IRSEI*** model while using only the ***AHP*** method.

	Ecological Factors					Weight	CI	RI	CR
	CVI	**WET**	**NDBSI**	**LST**	**DI**				
CVI	1	3	2	4	3	0.398			
WET	1/3	1	1/2	2	2	0.160			
NDBSI	1/2	2	1	3	2	0.242	0.023	1.12	0.021
LST	1/4	1/2	1/3	1	1/2	0.079			
DI	1/3	1/2	1/2	2	1	0.122			

CI is the consistency index; RI can be obtained by looking up the table. CR is the consistency ratio.

As can be seen from Table 3, the consistency ratio (***CR***) was 0.021, which was less than 0.1; thus, the results obtained have passed the consistency test, indicating that the calculated weights are reliable. Furthermore, by combining the ***PCA–AHP*** method, the weights (W_i) for the ***IRSEI*** model can be further fixed based on the minimum entropy. In conjunction with the five EEQ evaluation grades outlined in Table 1, the weights for the

proposed ***IRSEI*** model can be determined using Equation (11) to Equation (13), as listed in Table 4.

Table 4. The final weighs (***W***i) of the ***IRSEI*** model using the PCA–AHP method.

Factors	CVI	WET	NDBSI	LST	DI
Weights (Wi)	0.372	0.173	0.242	0.107	0.106

4.3. Results of Model Validation

As outlined in the model validation process (Section 3.3), 50 random samples were selected. These points were evenly distributed across the study area (Figure 4).

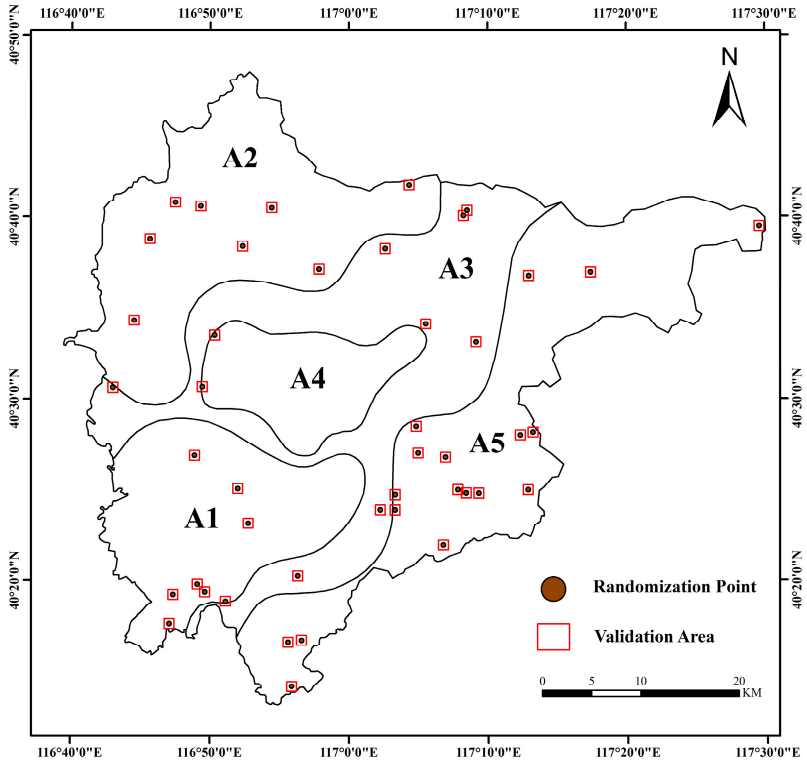

Figure 4. The distribution of the randomly selected field measurements using ***GE*** images. The symbols A1–A5 represent the five ecological function zones outlined in Section 2.2.

The accuracy of the evaluation results was verified using Google Earth images. The EEQ grades determined by the ***RSEI*** and ***IRSEI*** models were matched with the reference grades, and the details are illustrated in Table 5, where the overall accuracy for the ***RSEI*** and ***IRSEI*** models is 77.27% and 84.09%, respectively.

Table 5. Comparison of ***EEQ*** grades derived from the ***RSEI*** and ***IRSEI*** models.

Model	The Number of EEQ Grades That Matched the Reference Grades	Overall Accuracy (OA)
RSEI	34/44	77.27%
IRSEI	37/44	84.09%

A visual comparison of ***EEQ*** accuracy between the ***RSEI*** and ***IRSEI*** models, based on Google Earth imagery, is presented in Figure 5. The ***IRSEI*** model demonstrates a higher level of detail compared to the ***RSEI*** model.

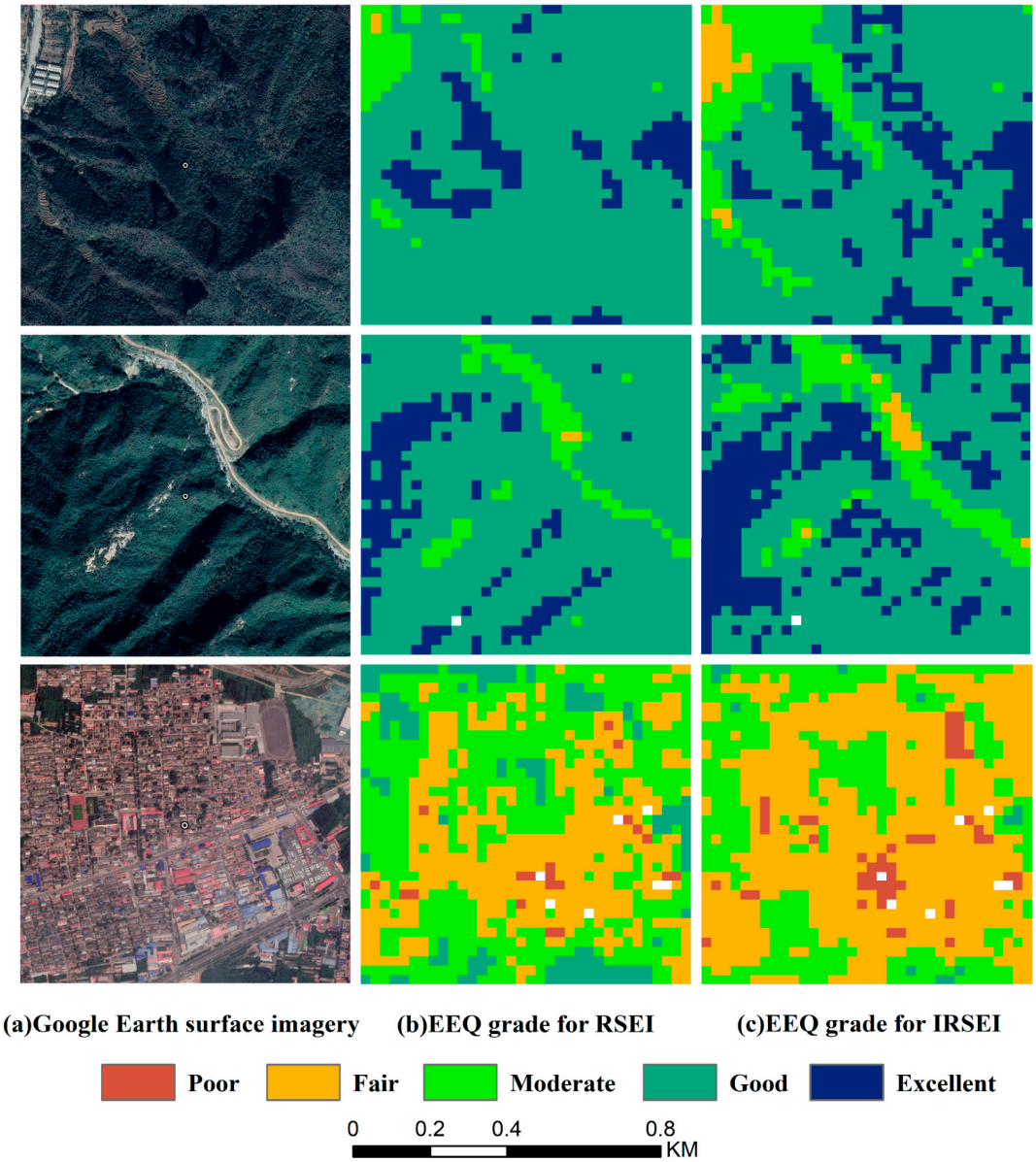

Figure 5. Visual interpretation on model validation using ***GE*** images.

To further evaluate the internal performance of the ***IRSEI*** model, the correlation coefficients between the various factors, as well as the coefficients between each calculated factor and the ***IRSEI*** model, are shown in Figures 6 and 7, respectively.

As can be seen from the figures, ***CVI*** and ***WET*** exhibit positive correlations with the actual values, while the remaining factors display negative correlations. Moreover, the proposed ***IRSEI*** model demonstrates a strong average correlation of 0.755, indicating its effectiveness in integrating key ecological factor information and outperforming individual factors in explaining ***EEQ***.

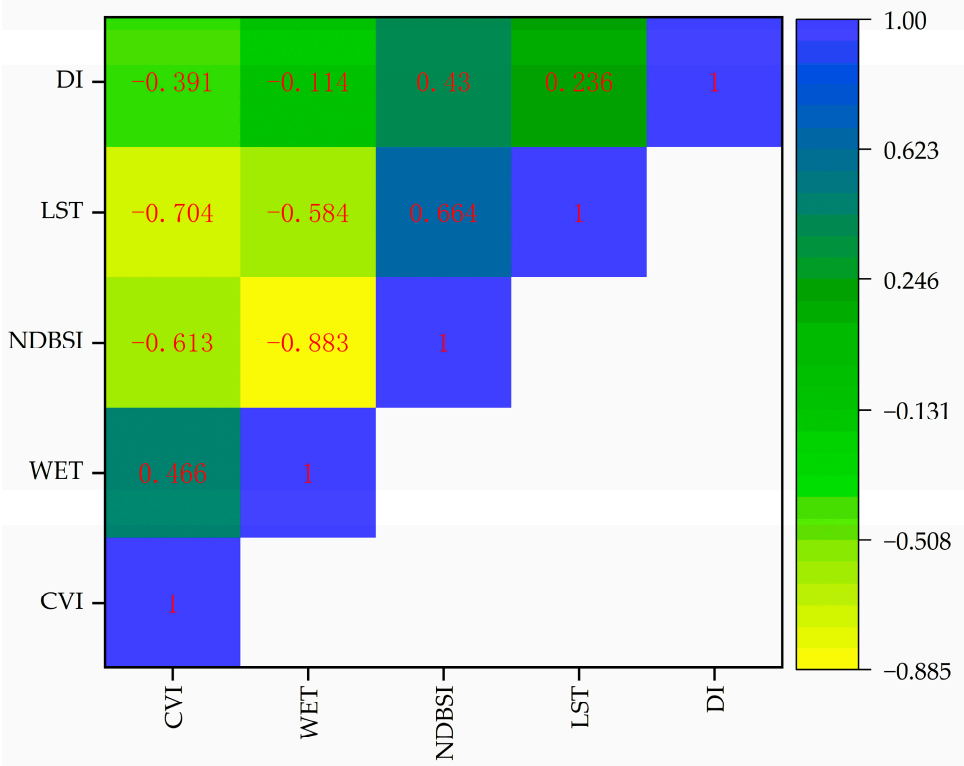

Figure 6. The correlation coefficients between the various factors.

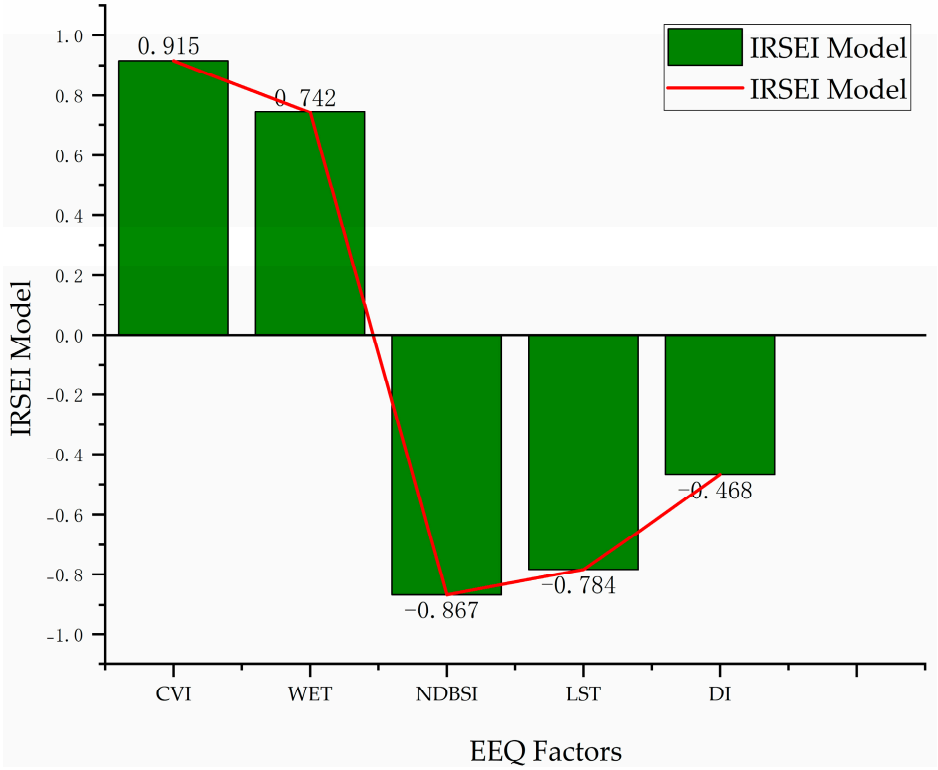

Figure 7. The coefficients between each EEQ factor and the ***IRSEI*** model.

4.4. Results of Model Application in Miyun

To evaluate the effectiveness and reliability of the proposed ***IRSEI*** model, the Miyun region was selected as a case study area. The model's performance was assessed through

EEQ evaluation (Section 4.4.1) and consistency analysis within the context of territorial spatial planning (Section 4.4.2).

4.4.1. Evaluation of Eco-Environmental Quality (*EEQ*)

With the acquired ***RSEI*** and ***IRSEI*** models, the results of ***EEQ*** can be mapped into five grades according to the criteria outlined in Section 3.3, as illustrated in Figure 8.

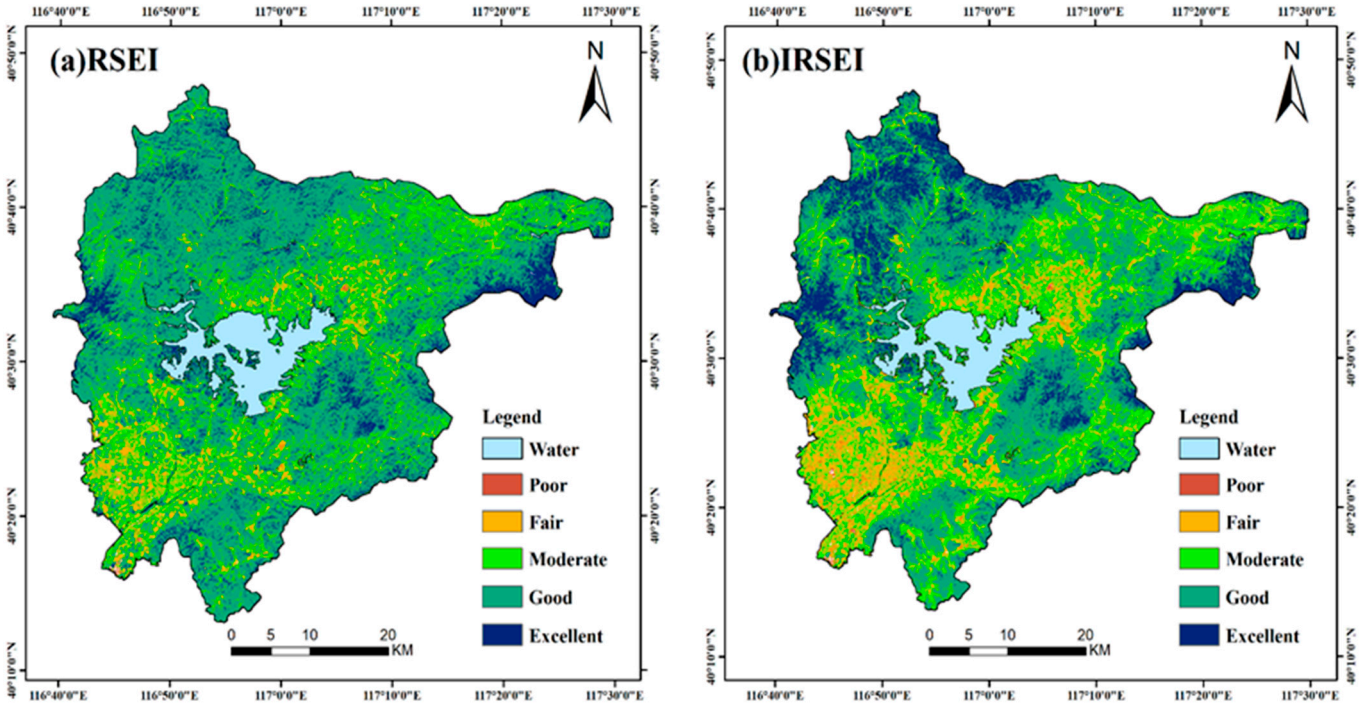

Figure 8. Map of the ***EEQ*** results using ***IRSEI*** and ***RSEI*** models.

As can be seen from Figure 8, the spatial distribution of ***EEQ*** by the two models is roughly the same. Regions with low ***EEQ*** values (poor) are concentrated in the southwest and northeast, while areas with good ***EEQ*** are predominantly located in the mountainous northwest and southeast. These findings align with existing knowledge of the region [56,57]. A graphical representation of the ***EEQ*** evaluation results is provided in Figure 9.

As shown in Figure 9, the general trends of urban ecological monitoring were similar, but there were differences in ecological levels. Notably, the most significant differences occur between the good and moderate categories. Despite identical grading standards, the ***IRSEI*** model can offer a more distinct ***EEQ*** classification. To further examine these model-specific ***EEQ*** discrepancies, an area transfer matrix (Table 6) was constructed.

Table 6. ***EEQ*** change the transfer matrix from ***RSEI*** to ***IRSEI***.

EEQ Grade		*IRSEI*				
		Poor	**Fair**	**Moderate**	**Good**	**Excellent**
RSEI	Poor	4.41	0.076			
	Fair	6.271	98.748	3.311		
	Moderate		121.076	319.154	63.118	
	Good			338.877	754.036	162.845
	Excellent			0.157	73.867	132.396

It can be seen from Table 6 that 62.97% of the ***EEQ*** evaluation results (diagonal line in the table) are the same, indicating that the evaluation results of ***IRSEI*** and ***RSEI*** are the same. In addition, 11.04% of the ***IRSEI*** areas (above the diagonal) are better than the ***RSEI***

areas, while 25.99% (below the diagonal) have deteriorated ecological grades. This shows that ***IRSEI*** is more sensitive to ***EEQ*** than ***RSEI***. A visual map of the ***EEQ*** change transfer matrix is illustrated in Figure 10.

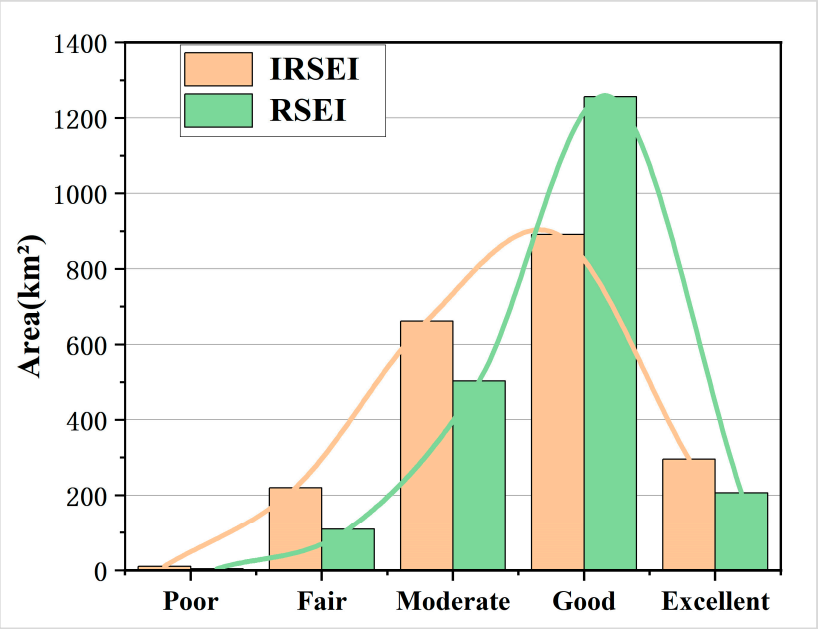

Figure 9. Visual and statistical comparison of EEQ results.

Figure 10 illustrates that regions experiencing ***EEQ*** improvement under the ***IRSEI*** model are primarily located in the mountainous northwest (40°30′N–40°48′N, 116°40′E–117°00′E) and southeast (40°20′N–40°30′N, 117°00′E–117°15′E), characterized by abundant vegetation and superior ***EEQ***. Conversely, areas exhibiting ***EEQ*** deterioration are concentrated in the urbanizing southwest and northeast, where rapid development and increased human impact have adversely affected the ecological environment.

4.4.2. Consistency Assessment in Territorial Spatial Planning

To verify the reliability of the proposed model, areas of EEQ results acquired by the ***IRSEI*** and ***RSEI*** models are spatially segmented and counted, as listed in Table 7.

As seen in Table 7, the ***EEQ*** grades from the ***IRSEI*** and ***RSEI*** display the same trend in different ecological functional zones (A1–A5), aligning well with the actual situation of the territorial spatial planning data in Miyun. The ecological function zone with the best ecological environment quality (***EEQ***) is A2 because it has high-vegetation coverage and the richest biomass, while the poorest ***EEQ*** is the comprehensive development core zone (A1) due to the most serious human interference. In addition, the zones A3, A4, and A5, designated as ecological protection areas by the government, demonstrate relatively good ***EEQ***. Furthermore, the ***EEQ*** statistical results obtained by ***IRSEI*** and ***RSEI*** models are visualized in Figure 11.

As can be seen from Figure 11, the statistical results across different ecological functional zones reveal significant differences in ***EEQ***. In the ecological function zone A2, the mean value of ***EEQ*** acquired from the proposed ***IRSEI*** model is 0.739, while ***RSEI*** is 0.713. In the poorest zone, A1, the mean values of ***EEQ*** calculated by the ***IRSEI*** and ***RSEI*** are 0.473 and 0.558, respectively. These results indicate that the ***EEQ*** achieved by the ***IRSEI*** is more effective and accurate than the ***RSEI*** model.

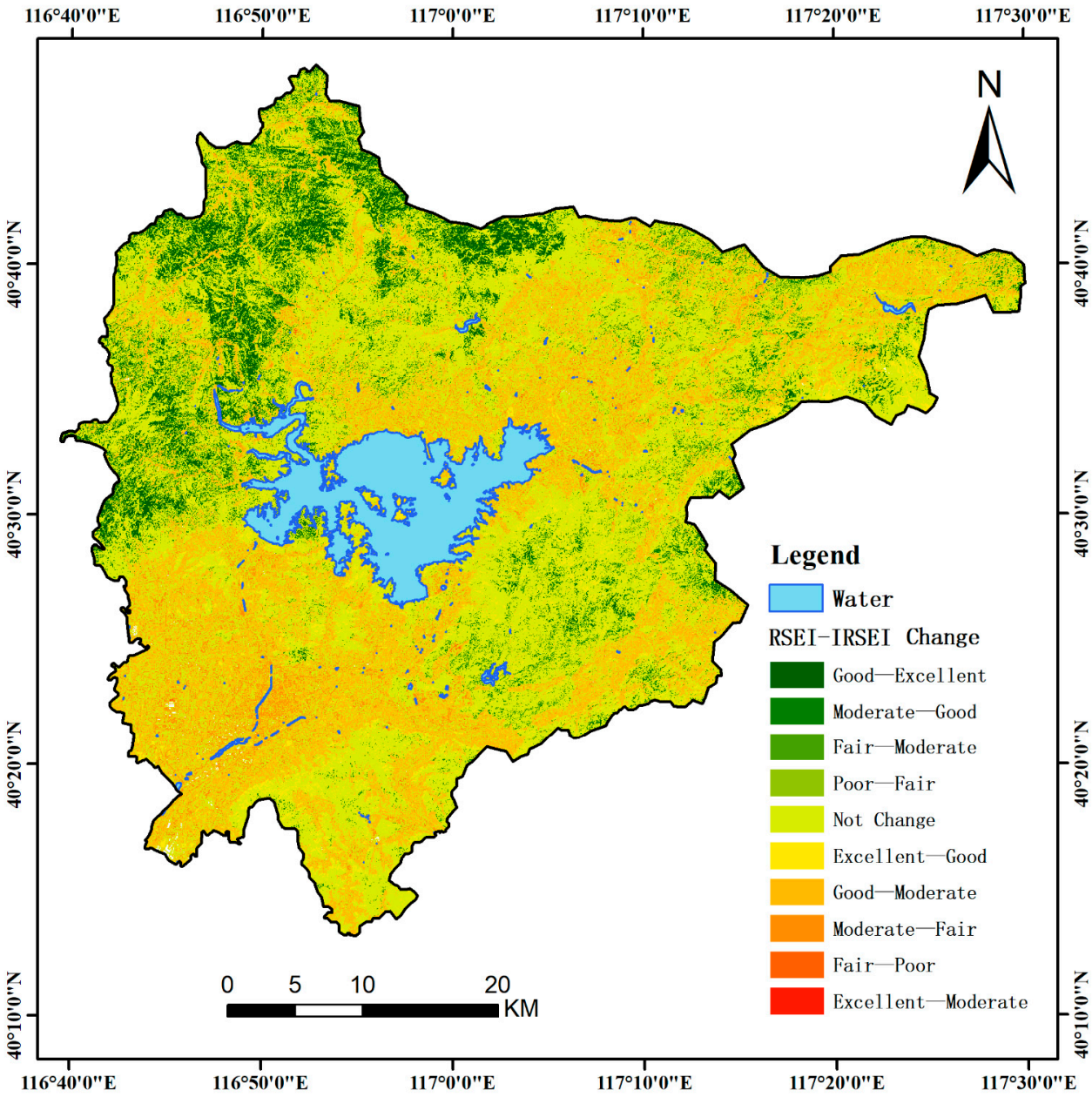

Figure 10. A map of the EEQ change transfer matrix.

Table 7. Area of EEQ grade in different ecological functional zones.

Zones	Models	Poor	Fair	Moderate	Good	Excellent
A1	IRSEI	6.651	113.56	171.783	69.435	3.071
	RSEI	2.941	59.13	145.638	142.868	13.924
A2	IRSEI	0.345	10.203	61.789	264.264	185.36
	RSEI	0.147	4.921	48.485	394.54	73.868
A3	IRSEI	0.059	3.852	26.536	26.337	6.107
	RSEI	0.024	0.964	13.511	41.489	6.899
A4	IRSEI	2.624	65.119	203.305	240.184	32.975
	RSEI	1.061	31.507	160.15	316.071	35.422
A5	IRSEI	0.695	25.348	196.223	288.886	72.348
	RSEI	0.23	10.706	131.989	360.203	80.373

A1–A5 are the five functional zones from the Territorial Spatial Planning (2017–2035) of Miyun.

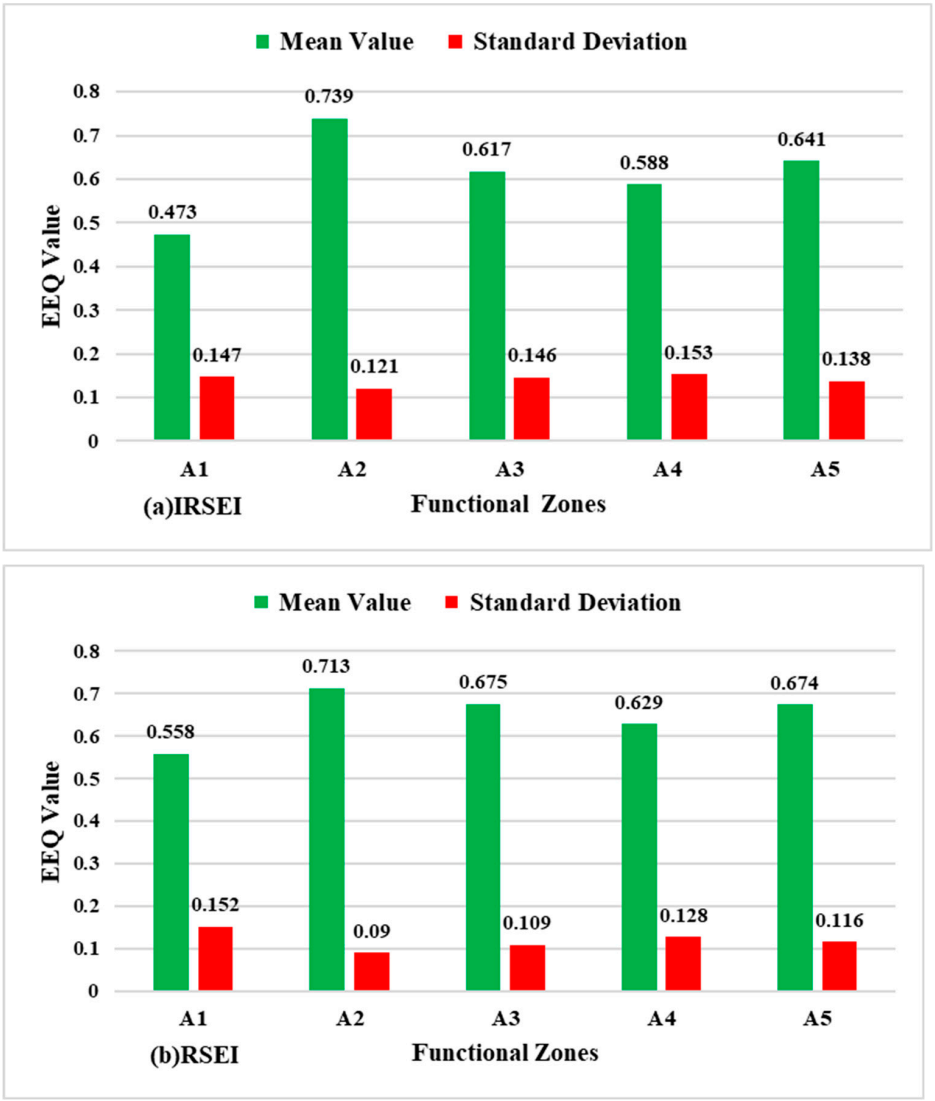

Figure 11. ***EEQ*** results were obtained by ***IRSEI*** and ***RSEI*** in different functional zones.

5. Discussion

5.1. Advantages of 3D Factors

In previous studies, 2D greenness indices are always created for the RSEI models [54]. These indices are the Normalized Difference Vegetation Index (***NDVI***) [58], Enhanced Vegetation Index (***EVI***) [23], Leaf Area Index (***LAI***) [59], Fractional Vegetation Cover (FVC) [60], and others. Different from these existing ***EEQ*** evaluation models that only use 2D ecological factors, the proposed ***IRSEI*** model introduces a new 3D ecological factor (***CVI***) in addition to 2D factors. The ***CVI*** factor can obtain vertical structural parameters of vegetation. Compared to the 2D ***NDVI*** factor, the 3D ***CVI*** factor that integrates vegetation canopy can more clearly distinguish between meadow and forest by values. Thus, higher ***CVI*** values were observed in forested areas, while lower values were found in urban and low-vegetation areas, as shown in Figure 3a,b. This is consistent with studies that tested in small areas [30]. Liu et al. [54] employed the method of multiplying the height of the vegetation canopy by the vegetation cover to calculate the three-dimensional greenness rate. Nonetheless, the three-dimensional greenness index is exclusively applicable to forested areas and lacks applicability to non-forested areas. Its contribution to evaluating the quality of the ecological environment is rather limited. Other 3D factors predominantly concentrate on small-area studies [30,61], utilizing methods such as airborne radar or ground-based scanners to acquire three-dimensional parameters of vegetation.

To intuitively understand the advantage of 3D ecological factors, three key areas (A1–A3) are selected and scaled to compare between 2D and 3D ecological factors, as illustrated in Figure 12.

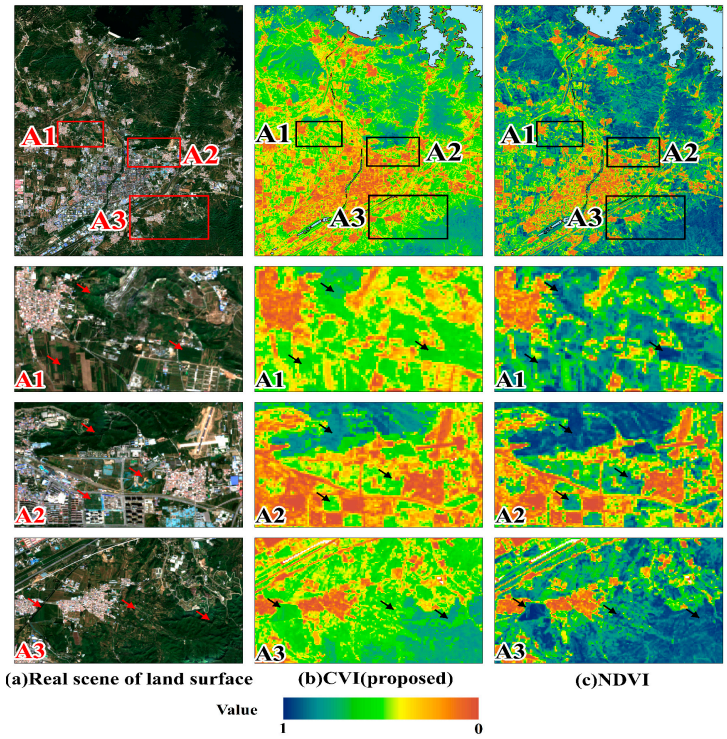

Figure 12. Comparison of ***EEQ*** results between the 3D factor (***CVI***) and 2D factor (***NDVI***).

As can be seen from Figure 12, the 3D ***CVI*** factor in the scaled areas (A1–A3) has a good discrimination ability for vegetation with different canopy heights and can distinguish woodlands, urban green spaces, and cultivated land with high-vegetation canopies to a large extent. The incorporation of 3D data into ***CVI*** effectively addresses the issue of saturation of remote sensing information when ecological factors are inverted through the sole use of optical remote sensing data [62]. This is consistent with the real-world observations, indicating that vegetation canopy height can effectively address the shortcomings of 2D EEQ factors, offering a more comprehensive representation of surface vegetation conditions. Therefore, the ***IRSEI*** model can transform ***EEQ*** evaluation from 2D to 3D and improve ***EEQ*** accuracy by introducing 3D factors.

5.2. Comparison of RSEI and IRSEI Models

The ***PCA*** has been widely used to determine the weights of ***EEQ*** models [63]. It is an adaptive method that may extract noise as a principal component [64], leading to unreliable results for some of the principal components. As listed in Table 2, the contributions of PC_1 to the ***RSEI*** model was 83.25%, while it was 68.169% to the proposed ***IRSEI*** model. In addition, the positive and negative values from PC_2 to PC_5 cannot explain ***EEQ***. Therefore, it is difficult to accurately characterize the regional ***EEQ*** using only PC_1, which contributes less [65–67].

To address this issue, a ***PCA–AHP*** hybrid weighting method was introduced, which can couple the weights of each factor based on the minimum entropy theory [68]. It avoids the subjective results inherent to the AHP-only approach and the instability of PC_1 contribution caused by only the ***PCA*** method [46], as listed in Table 4. Therefore, the ***PCA–AHP*** method emerges as a reliable approach for ***EEQ*** assessment.

Furthermore, to compare these two models, we have visualized the relationships between each ***EEQ*** model and its factors, as illustrated in Figure 13.

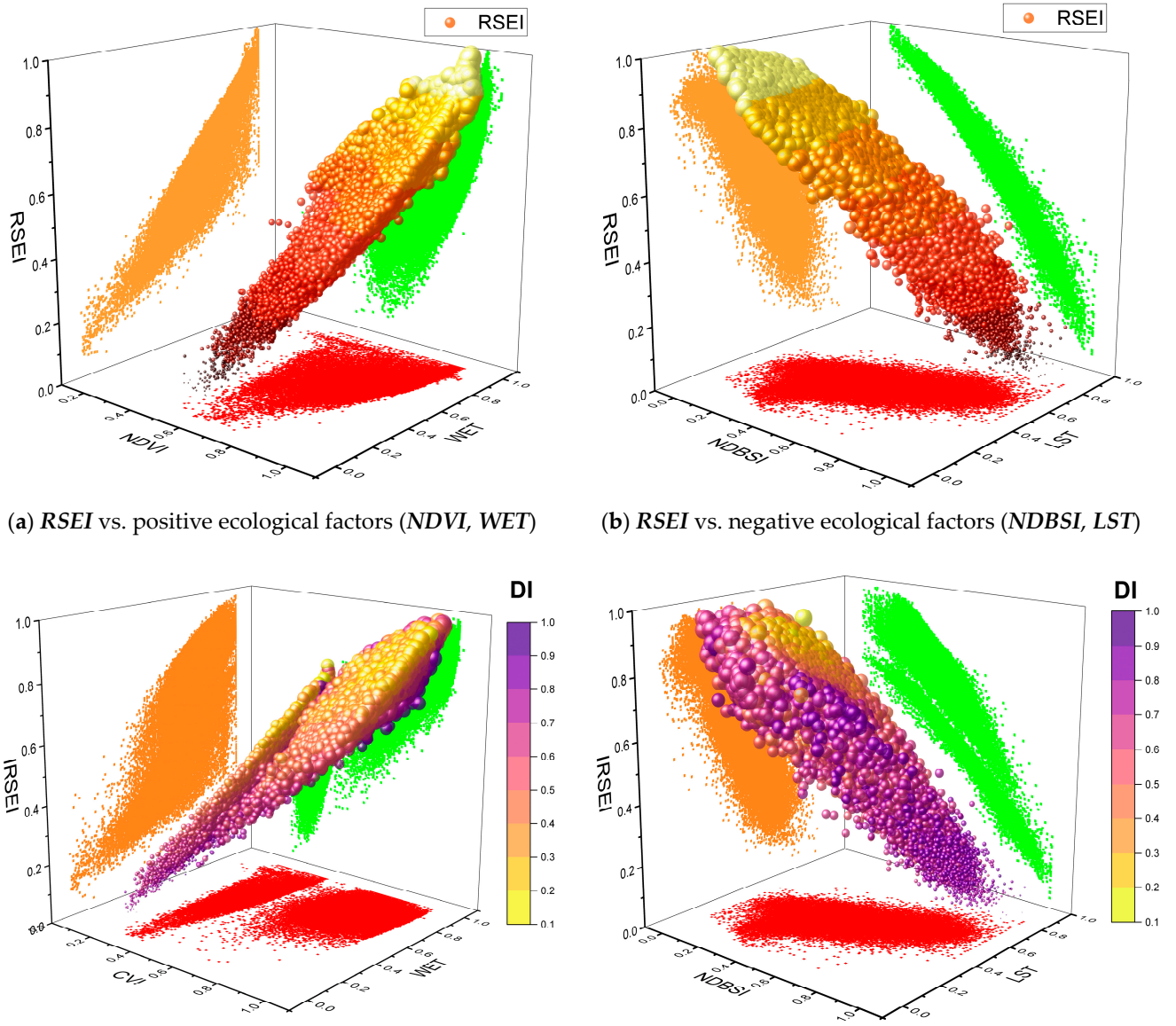

(**a**) ***RSEI*** vs. positive ecological factors (***NDVI***, ***WET***)

(**b**) ***RSEI*** vs. negative ecological factors (***NDBSI***, ***LST***)

(**c**) ***IRSEI*** vs. positive ecological factors (***CVI***, ***WET***)

(**d**) ***IRSEI*** vs. negative ecological factors (***NDBSI***, ***LST***, ***DI***)

Figure 13. The visualization of the relationship between each model and its ecological factors.

As illustrated in Figure 13, the ***IRSEI*** and ***RSEI*** models exhibit consistent patterns in the influence of key ecological factors on ***EEQ***. Specifically, ***NDVI*** and ***WET*** positively contribute to ***RSEI***, while ***NDBSI*** and ***LST*** negatively impact it. These findings align with previous studies [22,24,69]. Furthermore, the effect of ***CVI*** on the new ***IRSEI*** model was found to be greater than that of ***NDVI*** on the ***RSEI*** model, indicating that the vegetation factor (***CVI***), with the inclusion of 3D data, had a stronger explanatory power on the ecological environment [54]. The distribution of each ecological factor under different ***EEQ*** models was calculated (Figure 14).

It can be seen from Figure 14 that there is a significant difference in distribution between the two models. ***NDVI*** is mainly concentrated in the region of high values (0.6–1). The main reason is that ***NDVI*** exhibits low sensitivity in high-vegetation areas is low, which leads to saturation. This saturation effect makes it challenging to accurately differentiate between various vegetation types or conditions within these areas [54,62]. In contrast, ***CVI*** demonstrates a more balanced distribution with aggregations at both extremes. The reason for this is mainly that, after adding 3D data, ***CVI*** is more sensitive to vegetation compared to ***NDVI*** [30,54].

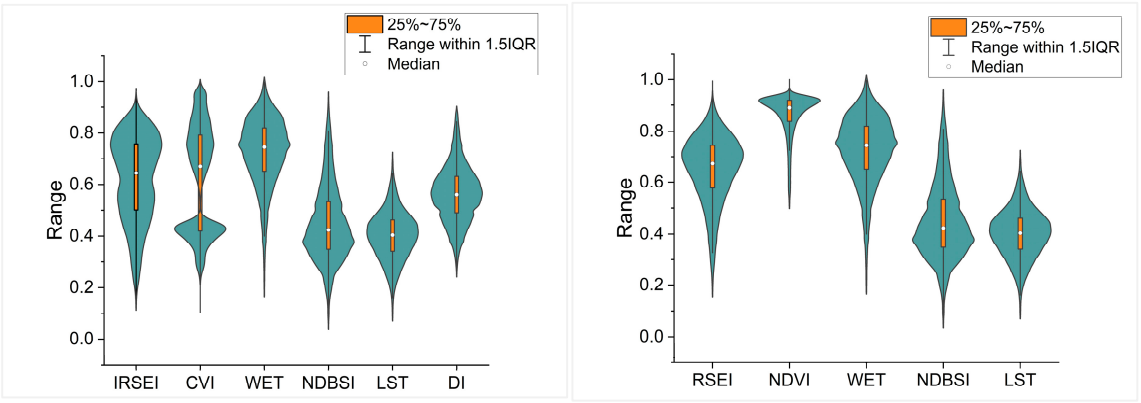

Figure 14. A visual summary of ecological factor distribution.

As seen in Figure 15, EEQ quantitatively reflected by the ***IRSEI*** model and remote sensing images is more consistent. For the monitoring of high-density contiguous built-up areas and high-vegetation coverage areas, the ***IRSEI*** model is more consistent with actual ecological environment conditions than ***RSEI***. In Figure 15(B1), for contiguous built-up areas, ***RSEI*** indicates that the ecological quality of these urban green spaces is too high. Contrastingly, ***IRSEI***, by adding 3D factors and increasing air quality factors, can more accurately monitor the ecological environment and avoid a higher ***EEQ*** setting. Consistent with the findings of Mao and Wang [70], who conducted a dynamic change analysis of ecological vulnerability in Miyun, the ***EEQ*** in the northwest forested area is significantly higher than in built-up areas. As seen in Figure 15(B2,B3), the integration of the 3D factor accentuates the disparity between ***RSEI*** and ***IRSEI*** in forest areas with high-vegetation cover. As expected, forest areas with high-vegetation cover exhibit superior ***EEQ*** compared to those with lower cover [71]. The ***IRSEI*** model effectively captures this relationship, demonstrating its ability to accurately represent ecological phenomena.

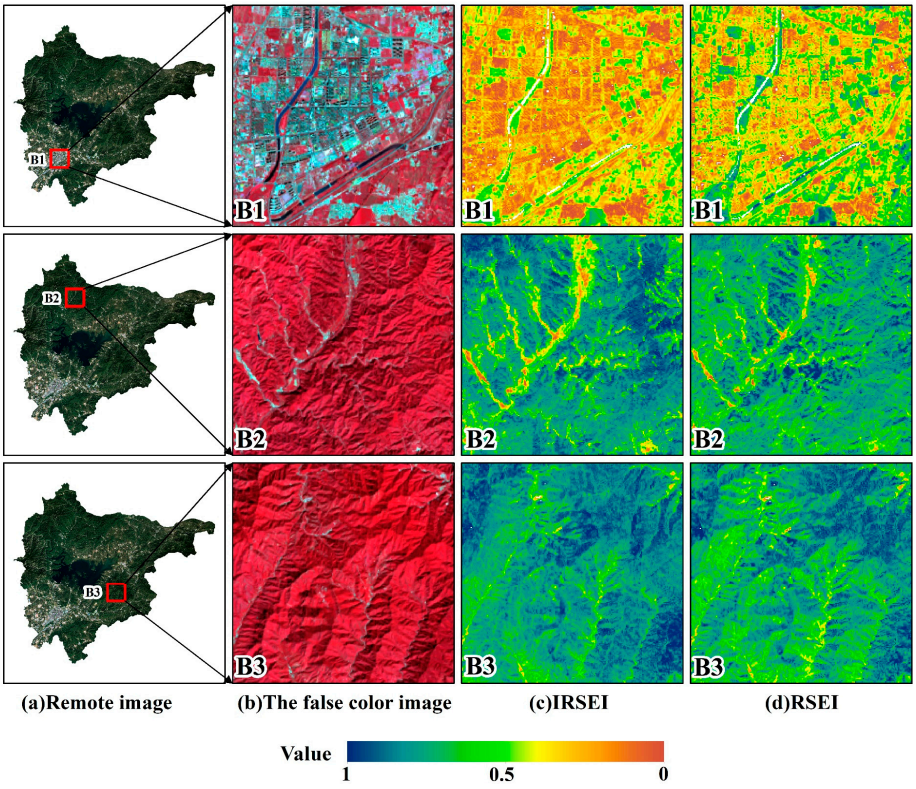

Figure 15. Comparison of ***EEQ*** results between the ***RSEI*** and ***IRSEI*** models.

6. Conclusions

In this research, a novel ***IRSEI*** model for large-scale ***EEQ*** assessment is proposed. It introduces air quality and 3D vegetation factors into the ***IRSEI*** framework and utilizes the PCA–AHP approach to determine optimal factor weights. Comprehensive experiments were conducted in an ecological support district. The results indicated that the proposed ***IRSEI*** model outperformed the existing ***RSEI*** model, and can achieve results that are more consistent with real-world ***EEQ*** conditions. The following conclusions were obtained from the experiment: (1) The difference index for the air quality factor can capture the changes in particle concentration, which is the chief pollutant of atmosphere pollution in Miyun, while the 3D vegetation factor can express the 3D canopy height. Consequently, the ***IRSEI*** model delivers more detailed ***EEQ*** assessments. (2) The ***PCA–AHP*** approach successfully balances objective and subjective information among the input ecological factors, thereby enhancing model stability and weight reliability.

In the future, more 3D ecological factors (e.g., building heights, and ***DEM***), natural and human factors (e.g., population density, road network density), and time series data need to be taken into consideration.

Author Contributions: Conceptualization, Y.L. and W.X.; methodology, Y.L. and W.X.; software, W.X. and P.G.; validation, Y.L., A.Z., P.H. and W.X.; resources, P.H.; data curation, W.X.; writing—original draft preparation, Y.L. and W.X.; writing—review and editing, P.H. and Y.L.; funding acquisition, Y.L. and P.H. All authors have read and agreed to the published version of the manuscript.

Funding: This work is jointly supported by the R&D Program of Beijing Municipal Education Commission (No. KM202410016006), the Fundamental Research Funds for Beijing University of Civil Engineering and Architecture (No. Y2207), the Pyramid Talent Training Project for Beijing University of Civil Engineering and Architecture (No. JDYC20220824), and the National Natural Science Foundation of China (No. 42001379).

Data Availability Statement: All data needed to replicate the conclusions in the paper are presented in the paper and the cited references.

Conflicts of Interest: The authors declare no conflicts of interest.

References

1. Chen, T.; Lu, Z.Y.; Yang, Y.; Zhang, Y.X.; Du, B.; Plaza, A. A Siamese Network Based U-Net for Change Detection in High Resolution Remote Sensing Images. *IEEE J. Sel. Top. Appl. Earth Obs. Remote Sens.* **2022**, *15*, 2357–2369. [CrossRef]
2. Zheng, X.X.; Chen, T. High spatial resolution remote sensing image segmentation based on the multiclassification model and the binary classification model. *Neural Comput. Appl.* **2023**, *35*, 3597–3604. [CrossRef]
3. Zhang, H.; Yin, Y.X.; An, H.M.; Lei, J.P.; Li, M.; Song, J.Y.; Han, W.H. Surface urban heat island and its relationship with land cover change in five urban agglomerations in China based on GEE. *Environ. Sci. Pollut. Res.* **2022**, *29*, 82271–82285. [CrossRef] [PubMed]
4. Chen, N.; Chen, Y.P.; Wang, Q.F.; Wu, S.P.; Zhang, H.Y. MAF-DeepLab: A Multiscale Attention Fusion Network for Semantic Segmentation. *Trait. Du Signal* **2022**, *39*, 407–417. [CrossRef]
5. Sun, C.; Li, J.L.; Liu, Y.C.; Cao, L.D.; Zheng, J.H.; Yang, Z.J.; Ye, J.W.; Li, Y. Ecological quality assessment and monitoring using a time-series remote sensing-based ecological index (ts-RSEI). *Giscience Remote Sens.* **2022**, *59*, 1793–1816. [CrossRef]
6. Tsai, Y.L.S.; Klein, I.; Dietz, A.; Oppelt, N. Monitoring Large-Scale Inland Water Dynamics by Fusing Sentinel-1 SAR and Sentinel-3 Altimetry Data and by Analyzing Causal Effects of Snowmelt. *Remote Sens.* **2020**, *12*, 3896. [CrossRef]
7. Yang, C.; Cai, X.B.; Wang, X.L. Remote Sensing of Hydrological Changes in Tian-e-Zhou Oxbow Lake, an Ungauged Area of the Yangtze River Basin. *Remote Sens.* **2018**, *10*, 27. [CrossRef]
8. Dallahi, Y.; Boujraf, A.; Meliho, M.; Orlando, C.A. Assessment of forest dieback on the Moroccan Central Plateau using spectral vegetation indices. *J. For. Res.* **2023**, *34*, 793–808. [CrossRef]
9. Yang, Y.L.; Wang, J.L.; Chen, Y.; Cheng, F.; Liu, G.J.; He, Z.H. Remote-Sensing Monitoring of Grassland Degradation Based on the GDI in Shangri-La, China. *Remote Sens.* **2019**, *11*, 3030. [CrossRef]
10. Du, Z.; Ji, X.; Liu, J.; Zhao, W.; He, Z.; Jiang, J.; Yang, Q.; Zhao, L.; Gao, J. Ecological health assessment of Tibetan alpine grasslands in Gannan using remote sensed ecological indicators. *Geo-Spat. Inf. Sci.* **2024**, *27*, 1–19. [CrossRef]
11. Ning, L.; Wang, J.Y.; Fen, Q. The improvement of ecological environment index model RSEI. *Arab. J. Geosci.* **2020**, *13*, 1866–7538. [CrossRef]
12. Liao, X.; Li, W.; Hou, J. Application of GIS Based Ecological Vulnerability Evaluation in Environmental Impact Assessment of Master Plan of Coal Mining Area. *Procedia Environ. Sci.* **2013**, *18*, 271–276. [CrossRef]

13. Cheng, J.N.; Zhao, K.X.; Li, H.; Tang, X.M.; Suo, Q.K. Dynamic changes and evaluation of land ecological environment status based on RS and GIS technique. *Trans. Chin. Soc. Agric. Eng. (Trans. CSAE)* **2008**, *24*, 83–88. (In Chinese)
14. Xu, S.; Bu, R.T.Y. Monitoring and evaluation of eco-environmental quality in Anhui Province in 2015 based on remote sensing. *Environ. Dev.* **2016**, *28*, 24–28. (In Chinese) [CrossRef]
15. Yue, A.; Zhang, Z. Research on analyzing changes in ecological status based on EI values. *J. Green Sci. Technol.* **2018**, *14*, 182+184. [CrossRef]
16. Ouyang, L.; Ma, H.Y.; Wang, Z.M.; Lu, C.Y.; Wang, C.L.; Zhang, Y.S.; Yu, X.S. Dynamic evaluation of ecological environment in Horqin sandy land based on remote sensing and geographic information data. *Acta Ecol. Sin.* **2022**, *42*, 5906–5921. [CrossRef]
17. Li, Y.C.; Yuan, J.G.; Liu, B.H.; Guo, H. Ecological Environment Dynamical Evaluation of Hutuo River Basin Using Remote Sensing. *Environ. Sci.* **2023**, *45*, 1–18. [CrossRef]
18. Xu, H.Q. A remote sensing index for assessment of regional ecological changes. *China Environ. Sci.* **2013**, *33*, 889–897. (In Chinese)
19. Shan, W.; Jin, X.; Ren, J.; Wang, Y.; Xu, Z.; Fan, Y.; Gu, Z.; Hong, C.; Lin, J.; Zhou, Y. Ecological environment quality assessment based on remote sensing data for land consolidation. *J. Clean. Prod.* **2019**, *239*, 118126. [CrossRef]
20. Hao, H.; Feifan, Y. Evaluation Of Spatial And Temporal Changes Of Mine Ecological Environment In Ili Valley Based On Remote Sensing Ecological Index. *J. Environ. Prot. Ecol.* **2022**, *23*, 2124–2132. [CrossRef]
21. Liu, Q.; Yu, F.H.; Mu, X.M. Evaluation of the Ecological Environment Quality of the Kuye River Source Basin Using the Remote Sensing Ecological Index. *Int. J. Environ. Res. Public Health* **2022**, *19*, 12500. [CrossRef]
22. Hu, X.S.; Xu, H.Q. A new remote sensing index for assessing the spatial heterogeneity in urban ecological quality: A case from Fuzhou City, China. *Ecol. Indic.* **2018**, *89*, 11–21. [CrossRef]
23. Zhang, P.P.; Chen, X.D.; Ren, Y.; Lu, S.Q.; Song, D.W.; Wang, Y.L. A Novel Mine-Specific Eco-Environment Index (MSEEI) for Mine Ecological Environment Monitoring Using Landsat Imagery. *Remote Sens.* **2023**, *15*, 933. [CrossRef]
24. Dong, C.Y.; Qiao, R.R.; Yang, Z.C.; Luo, L.H.; Chang, X.L. Eco-environmental quality assessment of the artificial oasis of Ningxia section of the Yellow River with the MRSEI approach. *Front. Environ. Sci.* **2023**, *10*, 1071631. [CrossRef]
25. Zhang, W.; Du, P.J.; Guo, S.C.; Lin, C.; Zheng, H.R.; Fu, P.J. Enhanced remote sensing ecological index and ecological environment evaluation in arid area. *Natl. Remote Sens. Bull.* **2023**, *27*, 299–317. [CrossRef]
26. Wang, Z.W.; Chen, T.; Zhu, D.Y.; Jia, K.; Plaza, A. RSEIFE: A new remote sensing ecological index for simulating the land surface eco-environment. *J. Environ. Manag.* **2023**, *326*, 116851. [CrossRef]
27. Song, M.J.; Luo, Y.Y.; Duan, L.M. Evaluation of Ecological Environment in the Xilin Gol Steppe Based on Modified Remote Sensing Ecological Index Model. *Arid. Zone Res.* **2019**, *36*, 1521–1527. [CrossRef]
28. Liu, Y.; Dang, C.Y.; Yue, H.; Lyu, C.G.; Qian, J.X.; Zhu, R. Comparison between modified remote sensing ecological index and RSEI. *Natl. Remote Sens. Bull.* **2022**, *26*, 683–697. [CrossRef]
29. Yang, X.Y.; Meng, F.; Fu, P.J.; Wang, Y.Q.; Liu, Y.H. Time-frequency optimization of RSEI: A case study of Yangtze River Basin. *Ecol. Indic.* **2022**, *141*, 109080. [CrossRef]
30. Zhang, Z.M.; Fan, Y.G.; Jiao, Z.J.; Fan, B.W.; Zhou, J.W.; Li, Z.H. Vegetation ecological benefits index (VEBI): A 3D spatial model for evaluating the ecological benefits of vegetation. *Int. J. Digit. Earth* **2023**, *16*, 1108–1123. [CrossRef]
31. Lai, S.H.; Sha, J.M.; Eladawy, A.; Li, X.M.; Wang, J.L.; Kurbanov, E.; Lin, Z.J.; Wu, L.B.; Han, R.; Su, Y.C. Evaluation of ecological security and ecological maintenance based on pressure-state-response (PSR) model, case study: Fuzhou city, China. *Hum. Ecol. Risk Assess.* **2022**, *28*, 734–761. [CrossRef]
32. Wang, Y.Q.; Wu, Z.J.; Yan, B.; Li, K.; Huang, F. Research on ecological environment impact assessment based on PSR and cloud theory in Dari county, source of the Yellow River. *Water Supply* **2021**, *21*, 1050–1060. [CrossRef]
33. Zhang, H.F.; Li, S.D.; Liu, Y.; Xu, M. Assessment of the Habitat Quality of Offshore Area in Tongzhou Bay, China: Using Benthic Habitat Suitability and the InVEST Model. *Water* **2022**, *14*, 1574. [CrossRef]
34. Wu, J.J.; Wang, X.; Zhong, B.; Yang, A.X.; Jue, K.S.; Wu, J.H.; Zhang, L.; Xu, W.J.; Wu, S.L.; Zhang, N.; et al. Ecological environment assessment for Greater Mekong Subregion based on Pressure-State-Response framework by remote sensing. *Ecol. Indic.* **2020**, *117*, 106521. [CrossRef]
35. Men, B.H.; Liu, H.Y. Water resource system vulnerability assessment of the Heihe River Basin based on pressure-state-response (PSR) model under the changing environment. *Water Sci. Technol.-Water Supply* **2018**, *18*, 1956–1967. [CrossRef]
36. He, J.H.; Huang, J.L.; Li, C. The evaluation for the impact of land use change on habitat quality: A joint contribution of cellular automata scenario simulation and habitat quality assessment model. *Ecol. Model.* **2017**, *366*, 58–67. [CrossRef]
37. Yu, J.B.; Li, X.H.; Guan, X.B.; Shen, H.F. A remote sensing assessment index for urban ecological livability and its application. *Geo-Spat. Inf. Sci.* **2022**, *27*, 289–310. [CrossRef]
38. Ashraf, A.; Haroon, M.A.; Ahmad, S.; Abowarda, A.S.; Wei, C.Y.; Liu, X.H. Use of remote sensing-based pressure-state-response framework for the spatial ecosystem health assessment in Langfang, China. *Environ. Sci. Pollut. Res.* **2023**, *30*, 89395–89414. [CrossRef]
39. Li, X.; Liu, Z.S.; Li, S.J.; Li, Y.X. Multi-Scenario Simulation Analysis of Land Use Impacts on Habitat Quality in Tianjin Based on the PLUS Model Coupled with the InVEST Model. *Sustainability* **2022**, *14*, 6923. [CrossRef]
40. Beijing Municipal Commission of Planning and Natural Resources. Available online: https://www.bjmy.gov.cn/zwgk/zfxxgk/fdzdgknr/ghxx/fzgh/201912/t20191227_129469.html (accessed on 27 December 2019).
41. United States Geological Survey. Available online: https://earthexplorer.usgs.gov/ (accessed on 25 April 2019).

42. Liu, X.Q.; Su, Y.J.; Hu, T.Y.; Yang, Q.L.; Liu, B.B.; Deng, Y.F.; Tang, H.; Tang, Z.Y.; Fang, J.Y.; Guo, Q.H. Neural network guided interpolation for mapping canopy height of China's forests by integrating GEDI and ICESat-2 data. *Remote Sens. Environ.* **2022**, *269*, 112844. [CrossRef]
43. Chan, A.H.Y.; Guizar-Coutino, A.; Kalamandeen, M.; Coomes, D.A. Reconstructing 34 Years of Fire History in the Wet, Subtropical Vegetation of Hong Kong Using Landsat. *Remote Sens.* **2023**, *15*, 1489. [CrossRef]
44. Laborde, H.; Douzal, V.; Pina, H.A.R.; Morand, S.; Cornu, J.F. Landsat-8 cloud-free observations in wet tropical areas: A case study in South East Asia. *Remote Sens. Lett.* **2017**, *8*, 537–546. [CrossRef]
45. Xu, H.Q.; Duan, W.F.; Deng, W.H.; Lin, M.J. RSEI or MRSEI? Comment on Jia et al. Evaluation of Eco-Environmental Quality in Qaidam Basin Based on the Ecological Index (MRSEI) and GEE. *Remote Sens.* **2022**, *14*, 2072–4292. [CrossRef]
46. Cheng, L.L.; Wang, Z.W.; Tian, S.F.; Liu, Y.P.; Sun, M.Y.; Yang, M.Y. Evaluation of eco-environmental quality in Mentougou District of Beijing based on improved remote sensing ecological index. *Chin. J. Ecol.* **2021**, *40*, 1177–1185. [CrossRef]
47. Xu, S.; Xu, D.; Liu, L. Construction of regional informatization ecological environment based on the entropy weight modified AHP hierarchy model. *Sustain. Comput. Inform. Syst.* **2019**, *22*, 26–31. [CrossRef]
48. Uddin, M.P.; Al Mamun, M.A.; Hossain, M.A. PCA-based Feature Reduction for Hyperspectral Remote Sensing Image Classification. *Iete Tech. Rev.* **2021**, *38*, 377–396. [CrossRef]
49. An, M.; Xie, P.; He, W.; Wang, B.; Huang, J.; Khanal, R. Spatiotemporal change of ecologic environment quality and human interaction factors in three gorges ecologic economic corridor, based on RSEI. *Ecol. Indic.* **2022**, *141*, 109090. [CrossRef]
50. Yu, L.; Gong, P. Google Earth as a virtual globe tool for Earth science applications at the global scale: Progress and perspectives. *Int. J. Remote Sens.* **2012**, *33*, 3966–3986. [CrossRef]
51. Yuan, Y.X.; Zhu, X.L.; Hou, C.H.; Liu, S.; Song, J.W.; Li, X.G. Spatiotemporal evolution characteristics and driving forces of surface thermal environment in mining intensive areas. *Sci. Technol. Eng.* **2022**, *22*, 14537–14548. (In Chinese)
52. Kucuker, D.M.; Giraldo, D.C. Assessment of soil erosion risk using an integrated approach of GIS and Analytic Hierarchy Process (AHP) in Erzurum, Turkiye. *Ecol. Inform.* **2022**, *71*, 101788. [CrossRef]
53. Gou, R.; Zhao, J. Eco-environmental quality monitoring in Beijing, China, using an RSEI-based approach combined with random forest algorithms. *IEEE Access* **2020**, *8*, 196657–196666. [CrossRef]
54. Liu, Y.; Xu, W.H.; Hong, Z.H.; Wang, L.G.; Ou, G.L.; Lu, N.; Dai, Q.L. Integrating three-dimensional greenness into RSEI improved the scientificity of ecological environment quality assessment for forest. *Ecol. Indic.* **2023**, *156*, 111092. [CrossRef]
55. Li, Y.; Wu, L.Y.; Han, Q.; Wang, X.; Zou, T.Q.; Fan, C. Estimation of remote sensing based ecological index along the Grand Canal based on PCA-AHP-TOPSIS methodology. *Ecol. Indic.* **2021**, *122*, 107214. [CrossRef]
56. Yan, S.J.; Wang, X.; Cai, Y.P.; Li, C.H.; Yan, R.; Cui, G.N.; Yang, Z.F. An Integrated Investigation of Spatiotemporal Habitat Quality Dynamics and Driving Forces in the Upper Basin of Miyun Reservoir, North China. *Sustainability* **2018**, *10*, 4625. [CrossRef]
57. Beijing Municipal Ecology and Environment Bureau. Beijing Ecology and Environment Statement 2019. Available online: https://sthjj.beijing.gov.cn/bjhrb/index/xxgk69/sthjlyzwg/1718880/1718881/1718882/index.html (accessed on 27 April 2020).
58. Kumar, B.P.; Babu, K.R.; Anusha, B.N.; Rajasekhar, M. Geo-environmental monitoring and assessment of land degradation and desertification in the semi-arid regions using Landsat 8 OLI/TIRS, LST, and NDVI approach. *Environ. Chall.* **2022**, *8*, 100578. [CrossRef]
59. Hu, Y.G.; Li, H.; Wu, D.; Chen, W.; Zhao, X.; Hou, M.L.; Li, A.J.; Zhu, Y.J. LAI-indicated vegetation dynamic in ecologically fragile region: A case study in the Three-North Shelter Forest program region of China. *Ecol. Indic.* **2021**, *120*, 106932. [CrossRef]
60. Wang, Z.; Bai, T.; Xu, D.; Kang, J.; Shi, J.; Fang, H.; Nie, C.; Zhang, Z.; Yan, P.; Wang, D. Temporal and Spatial Changes in Vegetation Ecological Quality and Driving Mechanism in Kökyar Project Area from 2000 to 2021. *Sustainability* **2022**, *14*, 7668. [CrossRef]
61. Gebremedhin, A.; Badenhorst, P.; Wang, J.; Giri, K.; Spangenberg, G.; Smith, K. Development and Validation of a Model to Combine NDVI and Plant Height for High-Throughput Phenotyping of Herbage Yield in a Perennial Ryegrass Breeding Program. *Remote Sens.* **2019**, *11*, 2494. [CrossRef]
62. Zhou, L.; Ou, G.; Wang, J.; Xu, H. Light saturation point determination and biomass remote sensing estimation of Pinus kesiya var. langbianensis forest based on spatial regression models. *Sci. Silvae Sin* **2020**, *56*, 38–47. [CrossRef]
63. Zhou, J.-L.; Xu, Q.-Q.; Zhang, X.-Y. Water Resources and Sustainability Assessment Based on Group AHP-PCA Method: A Case Study in the Jinsha River Basin. *Water* **2018**, *10*, 1880. [CrossRef]
64. Lever, J.; Krzywinski, M.; Altman, N. Points of significance: Principal component analysis. *Nat. Methods* **2017**, *14*, 641–643. [CrossRef]
65. Shan, W.; Jin, S.B.; Meng, X.S.; Yang, X.Y.; Xu, Z.G.; Gu, Z.M.; Zhou, Y.K. Dynamical monitoring of ecological environment quality of land consolidation based on multi-source remote sensing data. *Trans. Chin. Soc. Agric. Eng.* **2019**, *35*, 234–242. [CrossRef]
66. Hang, X.; Luo, X.Y.; Cao, Y.; Li, Y.C. Ecological quality assessment and the impact of urbanization based on RSEI model for Nanjing, Jiangsu Province, China. *Chin. J. Appl. Ecol.* **2020**, *31*, 219–229. [CrossRef]
67. Zheng, Z.C.; Chang, S.T.; Chen, W.H.; Wang, M.S.; Wu, S.J.; Chen, B.Q. Remote Sensing Monitoring and Evaluation of Ecological Environment Quality in Pingtan Comprehensive Experimental Area from 2007 to 2017. *J. Fujian Norm. Univ. (Nat. Sci. Ed.)* **2019**, *35*, 89–97. [CrossRef]
68. Zheng, Z.H.; Wu, Z.F.; Chen, Y.B.; Guo, C.; Marinello, F. Instability of remote sensing based ecological index (RSEI) and its improvement for time series analysis. *Sci. Total Environ.* **2022**, *814*, 152595. [CrossRef] [PubMed]

69. Xu, H.Q.; Wang, Y.F.; Guan, H.D.; Shi, T.T.; Hu, X.S. Detecting Ecological Changes with a Remote Sensing Based Ecological Index (RSEI) Produced Time Series and Change Vector Analysis. *Remote Sens.* **2019**, *11*, 2345. [CrossRef]
70. Mao, X.; Wang, H. Assessing ecological and environmental vulnerability of Miyun County in Beijing according to pixel scale. *J. Nanjing For. Univ.* **2017**, *60*, 96. [CrossRef]
71. Airiken, M.; Zhang, F.; Chan, N.W.; Kung, H.-t. Assessment of spatial and temporal ecological environment quality under land use change of urban agglomeration in the North Slope of Tianshan, China. *Environ. Sci. Pollut. Res.* **2022**, *29*, 12282–12299. [CrossRef]